

## Article

# New Corrosion Inhibitors Based on Perylene Units in Epoxy Ester Resin Coatings

Miroslav Kohl \*, Fouzy Alafid, Marek Bouška , Anna Krejčová, Yash Raycha, Andréa Kalendová, Radim Hrdina and Ladislav Burgert

Faculty of Chemical Technology, University of Pardubice, Studentská 573, 532 10 Pardubice, Czech Republic; fouzyramadanali.alafid@student.upce.cz (F.A.); marek.bouska@upce.cz (M.B.); anna.krejцова@upce.cz (A.K.); yash.raycha@student.upce.cz (Y.R.); andrea.kalendova@upce.cz (A.K.); radim.hrdina@upce.cz (R.H.); ladislav.burgert@upce.cz (L.B.)

\* Correspondence: miroslav.kohl@upce.cz; Tel.: +420-466-037-192

**Abstract:** Four new compounds from perylene dianhydride were prepared and tested for their anti-corrosion properties. Dizinc salt of perylene-3,4,9,10-tetracarboxylic acid and dimagnesium salts of perylene-3,4,9,10-tetracarboxylic acid, 5,5'-(1,3,8,10-tetraoxo-1,3,8,10-tetrahydroanthra[2,1,9-def:6,5,10-d'e'f'] diisoquinoline-2,9-diyl) bis(2-hydroxybenzoic acid) and *N,N'*-bis[3,3'-(dimethylamino)propylamine]-3,4,9,10-perylenediimide were characterized by analytical methods (SEM, EDX, X-ray) and parameters used in the field of paints (density, oil number and critical volume concentrations of pigment). The pigments (in a pigment volume concentration series) were used to prepare paints also containing a perylene C<sub>26</sub>H<sub>14</sub>N<sub>2</sub>O<sub>4</sub> (Compound I) derivative pigment plus inert titanium dioxide to maintain a constant concentration of solids in the paint film. A mixture containing zinc nitroisophthalate and both the perylene derivative and titanium dioxide served as the reference material. The paints were applied to steel panels in two layers with a ruler. The organic coatings were subjected to electrochemical measurements and accelerated cyclic corrosion tests. The highest corrosion resistance was found for the coating containing C<sub>24</sub>H<sub>8</sub>O<sub>8</sub>Mg<sub>2</sub>. Superior to the coating containing either C<sub>26</sub>H<sub>14</sub>N<sub>2</sub>O<sub>4</sub> or the conventional corrosion inhibitor C<sub>8</sub>H<sub>5</sub>N<sub>0</sub><sub>6</sub>-Zn, this pigment type acted mainly by a mechanism based on the compound's complexation capacity at the metallic surface/organic coating/corrosion medium interface. The organic coatings containing perylene acid salts also attained high mechanical resistance.

**Keywords:** perylene-3,4,9,10-tetracarboxylic acid salts; pigment; coating; corrosion; anticorrosion efficiency



**Citation:** Kohl, M.; Alafid, F.; Bouška, M.; Krejčová, A.; Raycha, Y.; Kalendová, A.; Hrdina, R.; Burgert, L. New Corrosion Inhibitors Based on Perylene Units in Epoxy Ester Resin Coatings. *Coatings* **2022**, *12*, 923. <https://doi.org/10.3390/coatings12070923>

Academic Editor: Matjaž Finšgar

Received: 31 May 2022

Accepted: 20 June 2022

Published: 29 June 2022

**Publisher's Note:** MDPI stays neutral with regard to jurisdictional claims in published maps and institutional affiliations.



**Copyright:** © 2022 by the authors. Licensee MDPI, Basel, Switzerland. This article is an open access article distributed under the terms and conditions of the Creative Commons Attribution (CC BY) license (<https://creativecommons.org/licenses/by/4.0/>).

## 1. Introduction

The application of organic coatings created from anticorrosion paints is the most common protection for metal materials. The method secures the chemical or electrochemical reaction of an anticorrosion pigment with the metal. Anticorrosion coatings are heterogeneous systems, and frequently consist of an organic binder with anticorrosion pigment particles dispersed in it [1–3]. An anticorrosion pigment is a power material that, added to an organic binder, exhibits corrosion-inhibiting effects. They frequently act by multiple corrosion-inhibiting mechanism types. In other words, the anticorrosion effect of the complex system of the anticorrosion pigment in the binder involves complex range of mechanisms [2,4,5]. A suitable combination of pigments with the binder is a prerequisite for anticorrosion properties to be at their optimum. Making use of the synergistic effect of two or more pigments is also a convenient option, selected depending on the aggressiveness of the medium [2,6]. Furthermore, the recommended (optimum) pigment concentrations (which are generally different for the different pigments) must also be adhered to [7]. In practice, phosphates, benzoates, chromates and other anions, including silicates are used as anodic corrosion inhibitors. The addition of these substances mainly affects the course

of the potential dependence of the partial anodic process. The action of anodic inhibitors often alkalifies the corrosive environment. Higher valence metal cations, oxo anions ( $\text{CrO}_4$ ,  $\text{MnO}_4$ ,  $\text{MoO}_4$ , and others), and nitrates are used as cathodic inhibitors. The action of these substances can be explained by the amplification of the partial cathodic process and its shift to the potential passivity region of the protected metal.  $\text{Ca}^{2+}$  and  $\text{Zn}^{2+}$  ions form mixed hydroxides with the corroding metal, which then block the cathodic sites. Similarly, polyphosphates block the cathodic process [8,9]. For a long time, lead compounds and chromate pigments have been used in paints as corrosion inhibitors for organic coatings. Various substitutes have been proposed for ecological variants with unsatisfactory results. Organic corrosion inhibitors instead of inorganic anti-corrosion pigments are not widely used, but organic inhibitors are sometimes used in combination with, for example, zinc phosphate pigment [10,11]. Organic inhibitors include organic amines, sulfonates and benzoates, and aromatic hetero compounds with nitrogen atoms, but also gelatin, tannin and glue. These inhibitors adsorb on the metal surface and prevent both anodic and cathodic reactions [12,13]. Organic pigments are generally extensive  $\pi$ -conjugated systems. Unlike inorganic corrosion inhibitors (magnesium azelate compounds with an active group containing nitrogen, sulfur and/or oxygen, which are used to sorb on the surface), organic anti-corrosion pigments are only sparingly soluble organic substances or metal salts of organic acids, and are used in binders in addition to inorganic pigments to enhance their function, especially in the initial phase of corrosion, and to create a synergistic effect. They were originally developed to replace toxic anti-corrosion pigments based on chromates and lead. Important organic anticorrosion pigments include zinc nitroisophthalate (Sicorin RZ), zinc-mercaptobenzothiazole, N-benzosulfonylanthranilic acids, and (2-benzothiazolylthio) succinic acid [11,14,15].

Materials referred to as perylene pigments include perylene-3,4,9,10-tetracarboxylic diimides, the chemical structure of which is described by the general formula (Figure 1a), where R is an aliphatic or an aromatic part (such as methyl or phenethylamine or 2,4-dimethylphenyl) [16,17].

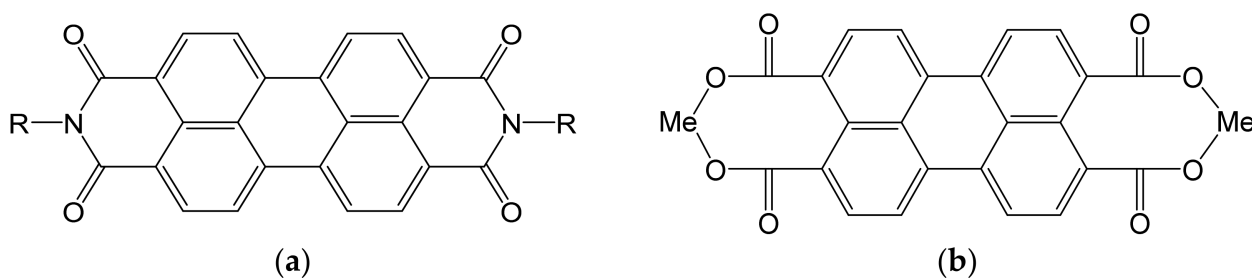


**Figure 1.** Chemical structure of Compounds: (a) Chemical structure of Compound I, III and IV; (b) Chemical structure of Compound II-Mg and II-Zn.

Organic pigments as such, including those perylene pigments that are normally used, are generally adequately or excellently weather resistant and light resistant but possess no anticorrosion properties [17,18]. This drawback can be obviated by adding certain corrosion inhibitor additives to the paint formula. However, such anticorrosion compounds have a chemical structure different from that of the pigment (color carrier), and thus are frequently structurally incompatible. Anticorrosion agents similar to the organic pigments are sought to eliminate this problem. The organic pigments are generally extensive  $\pi$ -conjugated systems, and so, for compatibility reasons, the anticorrosion compounds developed by us and described in this paper are also extensive  $\pi$ -conjugated systems, based on the perylene unit. Perylene-3,4,9,10-tetracarboxylic salts with the divalent cations of metals in the groups IIA or IIB of the periodic table can be generally described by the general formula (Figure 1b), where Me is the metal, i.e., Mg or Zn.

## 2. Materials and Methods

The dispersion agent MC-I (Figure 2) was obtained from the Faculty of Chemical Technology, University of Pardubice [19].

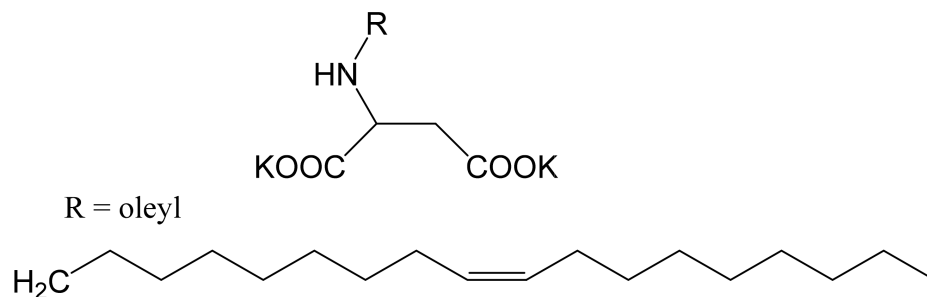


Figure 2. Dispersion agent MC-I structure.

Perylene-3,4,9,10-tetracarboxylic acid dianhydride, methylamine 40% and 5-aminosalicylic acid were obtained from Synthesia a.s., Pardubice, Czech Republic. Potassium hydroxide, zinc chloride, magnesium chloride hexahydrate and glacial acetic acid were obtained from Lach-ner, s.r.o. Neratovice, Czech Republic. Hydrochloric acid 35% and ethanol 96% were obtained from PENTA s.r.o. Prague, Czech Republic. *N,N*-dimethyl-1,3-propanediamine was obtained from Across Organic, Germany.

### 2.1. Synthesis of Compound I–IV

Since the commercial Pigment Red 179 contains various additives, we prepared pure Pigment Red 179 for the purposes of this study according to the procedure outlined in document [20]. Piperazine is used as a catalyst and surfactant in this process. Since the synthesis takes place in water in a heterogeneous phase (in suspension), in our synthetic procedure we replaced piperazine with the compound MC-I (potassium (*Z*)-octadec-9-en-1-ylaspartate), which acts as a catalyst and dispersant. This dispersant, together with the residual methylamine, is then removed from the product by thorough washing. Pigment Red 179 prepared in this way was tested according to standards CSN EN ISO 787-3 and CSN EN ISO 787-8 and it was shown that no extractable substances and water-soluble salts were released from the final dried pigment.

Pigment IV was synthesized in a very similar manner, except that the crude pigment after synthesis was purified by dispersion first in ethanol, then in alkaline water. It was finally washed with water.

#### 2.1.1. Synthesis of Compound I (C<sub>26</sub>H<sub>14</sub>N<sub>2</sub>O<sub>4</sub>; PR 179)

The synthesis of Pigment Red 179 can be described by the equation shown in Figure 3. The preparation from perylene-3,4,9,10-tetracarboxylic acid dianhydride is described, for example, in the literature procedures [21–23]. The compound I was synthesized following a procedure that was slightly modified from that described in the literature procedures for a similar PR179.

Perylene-3,4,9,10-tetracarboxylic acid dianhydride (24 g, 61.17 mmol) and dispersion agent MC-I (1 g, 1.7 mmol) were mixed with 320 cm<sup>3</sup> of water at room temperature (20 °C). Then, under intensive stirring, the temperature was increased at 90 °C and held at this temperature for 4 h. After that, the suspension was cooled to 23 °C and methyl amine (40% aqueous solution, 9.51 g, 310 mmol) was added dropwise over a period of 15 min. Once the addition was completed, the reaction mixture was stirred at 25 °C under a reflux condenser for another 45 min and then heated at 80 °C for 4 h. When the reaction was completed, the red pigment was filtered off, thoroughly washed with water (400 cm<sup>3</sup>) to remove excess amine, and dried at 80 °C.

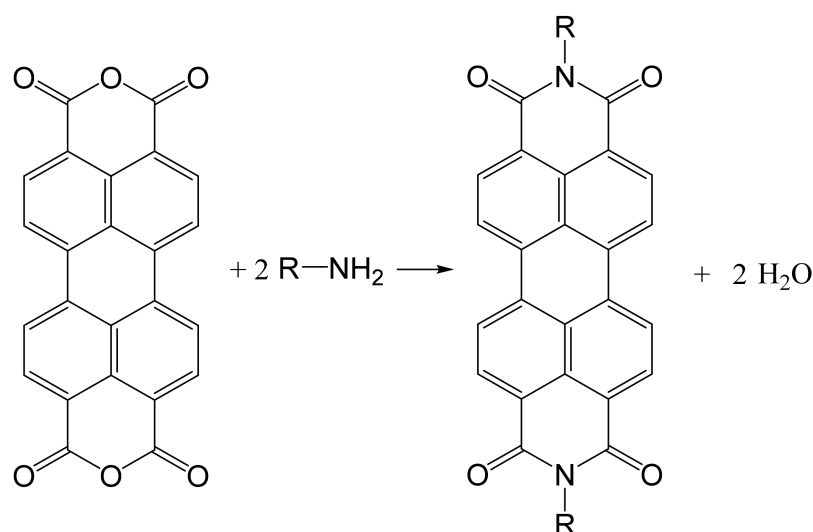


**Figure 3.** Synthesis of compounds I and IV.

The yield of red pigment ( $C_{26}H_{14}N_2O_4$ ;  $M_w = 418.4 \text{ g}\cdot\text{mol}^{-1}$ ; PR 179) was 24.33 g, i.e., 95% with respect to the initial perylene-3,4,9,10-tetracarboxylic acid dianhydride.

Elemental analysis:

Calculated: C, 74.64%; H, 3.37%; N, 6.70%.

Found: C, 73.96%; H, 3.27%; N, 6.73%.

#### 2.1.2. Synthesis of Perylene-3,4,9,10-tetracarboxylic Acid Salts

The synthesis of magnesium and zinc salts consisted of two reaction steps, which can be described by the equations shown in Figure 4.

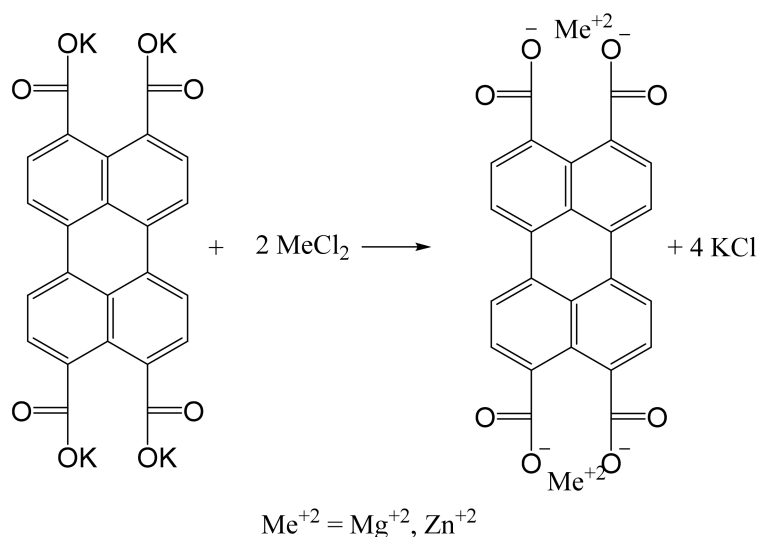


**Figure 4.** Synthesis of II-Zn and II-Mg compounds.

The preparation of the potassium salt of perylene-3,4,9,10-tetracarboxylic acid from perylene-3,4,9,10-tetracarboxylic acid dianhydride is described, for example, in the literature procedures [24,25]. The compounds II-Mg and II-Zn were synthesized following a procedure that was slightly modified from that described in the literature procedures.

#### 2.1.3. Synthesis of the Dimagnesium Salt of Perylene-3,4,9,10-tetracarboxylic Acid ( $C_{24}H_8O_8Mg_2$ ; II-Mg)

Perylene-3,4,9,10-tetracarboxylic acid dianhydride (5 g; 12.74 mmol) was mixed with 90 cm<sup>3</sup> of water. Aqueous KOH solution (47 cm<sup>3</sup>; 4.29 g, 76.4 mmol) was added and

the reaction mixture was stirred until a solution was formed. Then,  $\text{MgCl}_2 \cdot 6\text{H}_2\text{O}$  (5.44 g; 26.76 mmol) was added and the mixture was stirred at  $90^\circ\text{C}$  for 4 h. When the reaction was completed, the final pH value was 8. The formed yellow pigment was filtered off and the press cake was thoroughly washed with water ( $200\text{ cm}^3$ ). Finally, the pigment was dried at  $80^\circ\text{C}$ . The yield was 5.44 g, i.e., 90.2% with respect to the initial perylene-3,4,9,10-tetracarboxylic acid dianhydride.

The content of Mg in the prepared pigment ( $\text{C}_{24}\text{H}_8\text{O}_8\text{Mg}_2$ ) was  $101.01\text{ mg}\cdot\text{kg}^{-1}$ , and the theoretical amount was  $102.80\text{ mg}\cdot\text{kg}^{-1}$ .

#### 2.1.4. Synthesis of the Dizinc Salt of Perylene-3,4,9,10-tetracarboxylic acid ( $\text{C}_{24}\text{H}_{12}\text{O}_{10}\text{Zn}_2$ ; II-Zn)

The preparation was the same as in the case of the dimagnesium salt, except  $\text{ZnCl}_2$  (3.69 g; 27.06 mmol) was used instead of  $\text{MgCl}_2 \cdot 6\text{H}_2\text{O}$ .

The yield was 6.24 g, i.e., 82.8% with respect to the initial perylene-3,4,9,10-tetracarboxylic acid dianhydride.

The content of Zn in the prepared pigment ( $\text{C}_{24}\text{H}_{12}\text{O}_{10}\text{Zn}_2$ ) was  $213.7\text{ mg}\cdot\text{kg}^{-1}$ , and the theoretical amount was  $221.2\text{ mg}\cdot\text{kg}^{-1}$ .

#### 2.1.5. Synthesis of 5,5'-(1,3,8,10-Tetraoxo-1,3,8,10-tetrahydroanthra[2,1,9-def:6,5,10-d'e'f']) diisoquinoline-2,9-diyl)bis(2-hydroxybenzoic acid) ( $\text{C}_{38}\text{H}_{18}\text{N}_2\text{O}_{10}$ ; III)

The synthesis of compound III can be described by the equation shown in Figure 5. The preparation from perylene-3,4,9,10-tetracarboxylic acid dianhydride is described, for example, in the literature procedures [26–28]. Compound III was synthesized by our procedure which is described in document [29].

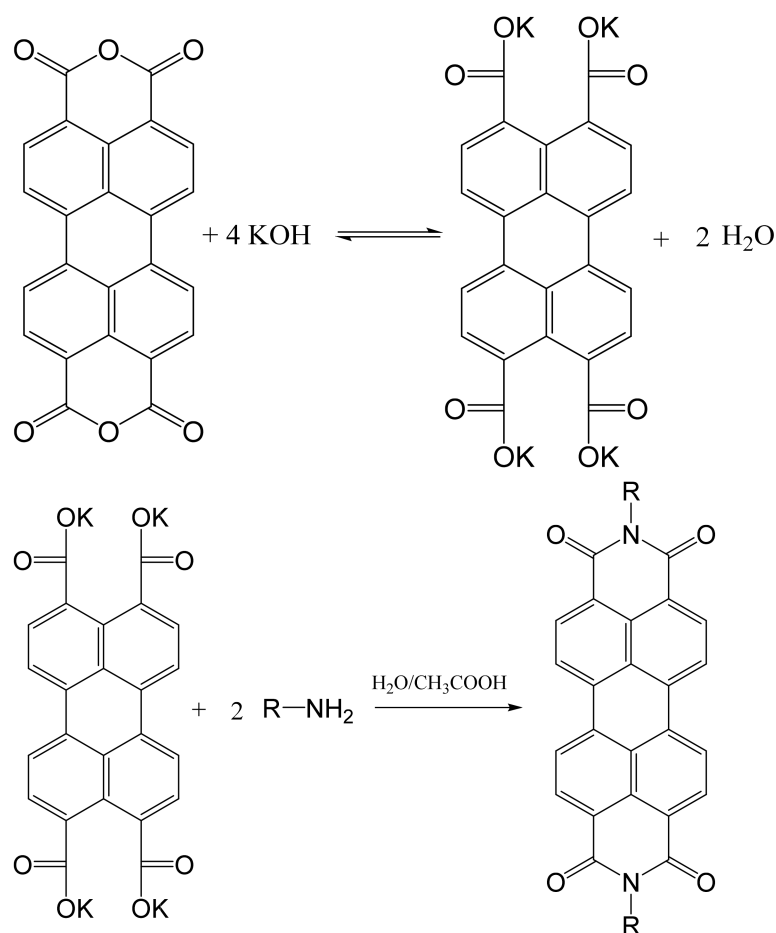


Figure 5. Synthesis of compound III.

Perylene-3,4,9,10-tetracarboxylic acid dianhydride (10 g, 25.4 mmol) and KOH (10 g, 175 mmol) were mixed with 175 cm<sup>3</sup> of water and stirred at 90 °C for 1 h. Then, the solution of potassium salt of perylene tetracarboxylic acid was cooled at 50 °C. Consequently, this solution was dropwise added to the mixture of glacial acetic acid (13.15 g, 12.5 cm<sup>3</sup>), 5-aminosalicylic acid (15.62 g, 101.9 mmol), and 50 cm<sup>3</sup> of water. The formed slurry was stirred at 50 °C for 20 min, and then the reaction mixture was poured into an autoclave where the reaction mixture was stirred at 160 °C for 23 h. When the reaction was completed, the pigment was filtered off and the press cake was stirred with water (400 cm<sup>3</sup>) for 30 min and the pH was adjusted to the value 2 using HCl (35%). Finally, compound III (C<sub>38</sub>H<sub>18</sub>N<sub>2</sub>O<sub>10</sub>; Mw 662.57 g·mol<sup>-1</sup>) was again filtered off, and the press cake was thoroughly washed with water (200 cm<sup>3</sup>) and dried at 80 °C. The yield was 14.85 g, i.e., 88% with respect to the initial perylene-3,4,9,10-tetracarboxylic acid dianhydride.

Elemental analysis:

Calculated: C, 68.89%; H, 2.74%; N, 4.23%.

Found: C, 67.04%; H, 2.77%; N, 4.21%.

#### 2.1.6. Synthesis of *N,N'*-Bis[3,3'-(dimethylamino) propylamine]-3,4,9,10-perylenediimide (C<sub>34</sub>H<sub>32</sub>N<sub>4</sub>O<sub>4</sub>; IV)

The synthesis of compound IV can be described by the equation shown in Figure 3. The preparation from perylene-3,4,9,10-tetracarboxylic acid dianhydride is described, for example, in the literature procedures [30,31]. Compound IV was also prepared by our procedure, which is described in document [29].

Dispersion agent MC-I (0.5 g) was mixed with 160 cm<sup>3</sup> of water; then, the pH was adjusted to 5 using HCl (35%) and perylene-3,4,9,10-tetracarboxylic acid dianhydride (11.20 g; 28.54 mmol) was added. The reaction mixture was stirred at 90 °C for 90 min. Then, the suspension was cooled at 50 °C and *N,N*-dimethyl-1,3-propanediamine (15.46 g, 150.7 mmol) was added dropwise over a period of 5 min to the reaction mixture. Once the addition was completed, the reaction mixture was stirred for another 20 min and poured into an autoclave where the reaction mixture was stirred at 160 °C for 23 h. Finally, the crude compound IV was filtered off, washed with water (200 cm<sup>3</sup>), and dried at 90 °C.

For purification purposes, the crude product was mixed with 200 cm<sup>3</sup> ethanol and intensively stirred at 55 °C for 30 min. Then, the crude product was filtered off and washed with ethanol (200 cm<sup>3</sup>). After that, the press cake was mixed with 200 cm<sup>3</sup> of aqueous solution of KOH (3%) and intensively stirred at 65 °C for 30 min. Finally, compound IV (C<sub>34</sub>H<sub>32</sub>N<sub>4</sub>O<sub>4</sub>; Mw 560.65 g·mol<sup>-1</sup>) was filtered off and washed with water (300 cm<sup>3</sup>). The yield was 13.64 g, i.e., 85.3% with respect to the initial perylene-3,4,9,10-tetracarboxylic acid anhydride.

Elemental analysis:

Calculated: C, 72.84%; H, 5.75%; N, 9.99%.

Found: C, 73.08%; H, 5.80%; N, 9.66%.

The synthesis of the dimagnesium salt of perylene-3,4,9,10-tetracarboxylic acid (C<sub>24</sub>H<sub>8</sub>O<sub>8</sub>Mg<sub>2</sub>; compound II-Mg) and the synthesis of the dizinc salt of perylene-3,4,9,10-tetracarboxylic acid (C<sub>24</sub>H<sub>12</sub>O<sub>10</sub>Zn<sub>2</sub>; compound II-Zn) were carried out with the aim of preparing new compounds containing Mg<sup>2+</sup> or Zn<sup>2+</sup> cations, which due to their structure and type of selected cation were expected to have anti-corrosion effects [15,29]. The synthesis of 5,5'-(1,3,8,10-tetraoxo-1,3,8,10-tetrahydroanthra[2,1,9-def:6,5,10-d'e'f']) diisoquinoline-2,9-diylbis(2-hydroxybenzoic acid) (C<sub>38</sub>H<sub>18</sub>N<sub>2</sub>O<sub>10</sub>; compound III) and the synthesis of *N,N'*-bis[3,3'-(dimethylamino)propylamine]-3,4,9,10-perylenediimide (C<sub>34</sub>H<sub>32</sub>N<sub>4</sub>O<sub>4</sub>; compound IV) were performed so that the compounds contained a free electron nitrogen pair. The anions of these dissociated compounds were assumed to have an affinity for the positively charged corrosion center. Complementarily, compounds were prepared which contained an acidic group in their structure.

## 2.2. Analytical Methods and Equipment

Elemental analysis was performed by standard procedures with the analyzer from the Fisons Instrument. The determination of magnesium and zinc was carried out using inductively coupled plasma–optical emission spectroscopy (ICP-OES). The sample was decomposed in a microwave mineralizer Speedwave Xpert (Berghof, Tübingen, Germany). The sample was weighed precisely 0.1 to 0.2 g; after that, 7 mL of nitric acid (Penta Chrudim, Czech Republic, purity PP) was added and then the sample was left to react for 20 min in an open vessel, after which it was decomposed (170 °C for 15 min, 200 °C for 20 min). Finally, the mineralized sample was made up to a volume of 50 mL.

The determination of both elements in the mineralized sample was performed using an inductively coupled plasma optical emission spectrometer Integra 6000 (GBC, Dandenong, Victoria, Australia) equipped with a concentric nebulizer and cyclonic spray chamber (both Glass Expansion, Melbourne, Victoria, Australia) at the spectral lines of Mg II 280.270 nm and Zn I 213.856 nm. Working conditions for ICP-OES analysis were as follows: a sample flow rate of 1.5 mL·min<sup>-1</sup>; the plasma power 1000 W; plasma, external and sample gases 10, 0.6 and 0.65 L·min<sup>-1</sup>; observation height 6.5 mm and three repeated measurements at 1 s were used to read the signal and fixed background correction. Calibration standards 10, 5, 1, 0.5 to 0.1 mg·dm<sup>3</sup> were prepared from commercially available standard solutions of zinc and magnesium 1 g·dm<sup>-3</sup> (SCP, Science, Clark Graham, Baie D'Urfé, QC, Canada). The limits of detection (concentration equivalent to three times the standard deviation of noise in the place of background correction) for both elements were around 2 µg·dm<sup>-3</sup>, while the limit of detection for the whole analytical procedure, with respect to the preparation of the sample for analysis (sample weight 0.05 g and 50 mL), was 2 mg·kg<sup>-1</sup>.

### 2.2.1. SEM

Samples were photographed using the electron microscope JSM7500F. The accelerating voltage of the primary electron beam was 5 kV. The surface of the samples was destroyed by sputtering a thin layer of gold.

### 2.2.2. EDX Measurement

EDX measurements are in wt%. Morphology and chemical compositions of pigments were studied using scanning electron microscopy (SEM, TESCAN, VEGA 3, EasyProbe, Brno, Czech republic) linked with an energy-dispersive X-ray spectroscopic analyzer (EDX). Standard uncertainties of EDX measurements were ±1 at.%. Typically, the EDX measurements were performed at 3 spots per sample and averaged.

### 2.2.3. X-ray Diffraction

A D8 ADVANCE X-ray diffractometer (Bruker AXS, Karlsruhe, Germany) equipped with a vertical  $\Theta$ - $\Theta$  goniometer (radius = 217.5 mm) was used to measure the powder diffractograms.

The goniometer was equipped with an X-ray tube with a Cu anode (U = 40 kV, I = 30 mA;  $\lambda = 1.5418 \text{ \AA}$ ), a graphite secondary monochromator, and a scintillation Na(Tl)I detector. The measurement was performed at room temperature in the range of 2–50° (2 $\Theta$ ) with a step of 0.02° and the reading time of the diffracted radiation intensity was 5 s/step.

## 2.3. Characterization of the Pigment and Binder

### 2.3.1. Pigment Parameter Determination

The specifications of pigments which were taken into consideration were oil absorption, density, PVC, and CPVC. Density and oil absorption were determined using a Micromeritics AutoPycnometer 1340 (Norcross, GA, USA) and “pestle–mortar” method based on the Czech Standard CSN 67 0531, respectively. While collecting these data, CPVC was calculated.

### 2.3.2. Specification of the Binder for Coatings

The binder used, by its trade name, was Worlee D 46 epoxy ester resin. Its specification was as follows: solids—60%; acid value—4; and viscosity—2.5–5.0 Pa·s.

### 2.4. Formulation and Preparation of the Organic Coatings

The synthesized perylene pigments ( $C_{38}H_{18}N_2O_{10}$ ,  $C_{34}H_{32}N_4O_4$ ,  $C_{24}H_8O_8Mg_2$ ,  $C_{24}H_{12}O_{10}Zn_2$ ), titanium dioxide ( $TiO_2$ ), and zinc salt of nitrosophthalic acid ( $C_8H_5NO_6-Zn$ ) were used to prepare the paints (organic coatings). A solvent-based epoxy ester resin was used as the binder. The organic coatings were formulated at a perylene derivative pigment volume concentration of PVC = 1%, using perylenic acid salts ( $C_{38}H_{18}N_2O_{10}$ ,  $C_{34}H_{32}N_4O_4$ ,  $C_{24}H_8O_8Mg_2$ , and  $C_{24}H_{12}O_{10}Zn_2$ ) at PVC = 0.1%, 0.2% and 0.35%, and zinc nitroisophthalate ( $C_8H_5NO_6-Zn$ ) at PVC = 0.1%. The model paints were also pigmented with  $TiO_2$  to maintain a constant concentration of solids so that the pigment volume concentration to critical pigment volume concentration ratio was PVC/CPVC = 0.02. Furthermore, two model paints were formulated: one with the perylene derivative at PVC = 1% and  $TiO_2$  at PVC/CPVC = 0.02, and one with  $TiO_2$  at PVC/CPVC = 0.02 solely. The paints were prepared using a Dissolver-type system at 3500 rpm/30 min. After synthesis, the application of these coatings was performed on steel panels (standard S-46 and S-36 low-carbon steel panels, Q-Lab Corporation). The dry film thickness of the coatings was measured with a magnetic gauge according to ISO 2808.

### 2.5. Corrosion Test Procedures

#### 2.5.1. Accelerated Cyclic Corrosion Test in an Atmosphere of $SO_2$ with Water Condensation (ISO 6988)

This test consists of subjecting the samples for 24 h:8 h to  $SO_2$  at a temperature of 38 °C (1 L  $SO_2$  is injected into a 300 L chamber), followed by exposure to the condensation of humidity for a period of 16 h at a temperature of 21 °C. Results were observed after 960 h.

#### 2.5.2. Accelerated Cyclic Corrosion Test in an Atmosphere of NaCl with Water Steam Condensation (ISO 9227)

Samples were subjected to 12 h cycles divided into three parts: 6 h of exposure to a mist of 5% solution of NaCl at a temperature of 35 °C; 2 h of exposure at a temperature of 23 °C; and 4 h of humidity condensation at a temperature of 40 °C. The tests ended after 1440 h.

#### 2.5.3. Accelerated Cyclic Corrosion/Weather Resistance Test with Exposure to a Salt Electrolyte and UV Radiation

In this testing chamber, the samples were subjected to 12 h cycles divided into three parts: 10 h of exposure to a mist of 0.05% solution of NaCl + 0.35% solution of  $(NH_4)_2SO_4$  at a temperature of 35 °C; 1 h of exposure at a temperature of 23 °C; and 1 h of humidity condensation at a temperature of 40 °C. The samples were evaluated after 168 h of exposure. After that, for the UV test, the samples were exposed in a fluorescent UV/condensation chamber in 12 h cycles divided into two parts: the first 8 h involved exposure to UV radiation at 60 °C (by using UVA-340 discharge lamps) followed by 4 h of exposure to moisture at 50 °C. The samples were evaluated after 168 h of operation. The whole test was repeated thrice so that the total exposure time was 1008 h. The procedure was derived from ASTM D 5894-96.

#### 2.5.4. Evaluation of Results after Corrosion Tests

Results of the corrosion tests were finalized as specified in the following standards. The ASTM D 714-87 standard describes blistering on the paint film surface; thus, blistering on sample paint film was inspected by comparison with the standard. Corrosion on the metal plate was evaluated (after stripping the paint film down) by comparison with the photographs of standards included in the ASTM D 610-85 standard [32].



## 2.6. Potentiodynamic Polarization Studies

The electrochemical test of linear polarization was conducted using a VSP-300 multichannel potentiostat/galvanostat (Bio-Logic, Seyssinet-Pariset, France). In the three-electrode setting, 1 cm<sup>2</sup> of the sample was submerged in a 1 M NaCl solution and polarized across the range from  $-10 \text{ mV } E_{OC}^{-1}$  to  $+10 \text{ mV } E_{OC}^{-1}$  at and rate of  $0.166 \text{ mV s}^{-1}$ . The spontaneous corrosion potential ( $E_{corr}$ ), corrosion current density ( $I_{corr}$ ), polarization resistance ( $R_p$ ), and corrosion rate ( $v_{corr}$ ) were measured when the polarization procedure was over. The measurement was repeated after 480 h of exposure of the samples to an atmosphere of SO<sub>2</sub> with water condensation.

From this technique, polarization resistance  $R_p$  of a material and  $I_{corr}$  can be determined. Polarization resistance is defined as the resistance of the specimen to oxidation during the application of an external potential. The formula is the inverse of the slope of the current density vs. the potential curve at free corrosion potential (at which the overpotential  $dE \rightarrow 0$ ). The polarization resistance is described by the relation in Equation (1) [33].

$$R_p = \frac{1}{\frac{dI}{dE}} dE \rightarrow 0 \quad (1)$$

Alternatively, it can be understood as the slope of a potential vs. current density line within the zero current point,  $I = 0$ . The rate of polarization should be close to zero. The polarization resistance value is then used to calculate the corrosion rate in the form of the corrosion current density ( $I_{corr}$ ) using Equation (2).

$$I_{corr} = \frac{B}{R_p} \quad (2)$$

However, for coefficient  $B$  (the Stern–Geary coefficient), the Tafel slopes  $\beta_a, \beta_c$  must be known for Equation (3). The Tafel slopes  $\beta_a, \beta_c$  are obtained by evaluating the polarization curve [34,35].

$$B = \frac{\beta_a \beta_c}{2.303 (\beta_a + \beta_c)} \quad (3)$$

Parameters found by this method can be used to calculate the corrosion rate using the relationship Equation (4) [36]:

$$v_{corr} = \frac{I_{kor} M t}{\rho z F} \quad (4)$$

## 2.7. Mechanical Properties of the Paints

For the mechanical properties of paint films, elasticity and strength were analyzed. ISO 2409 describes cutting a lattice into the film using a special cutting blade with cutting edges 2 mm apart for the adhesion test. The impact strength of the paint films applied to steel panels was determined by letting a 1000 g weight fall onto the panels from different heights and recording the largest height (in mm) at which the film could bare the impact without damage (ISO 6272). An Erichsen cupping test was used to test the paint film's resistance to cupping. The result was the steel ball indentation depth (in mm) at which the film integrity remained undisturbed, as specified in ISO 1520. The elasticity of paint film was examined by the mandrel test, in which the panels were bent over mandrels of different diameters. The largest diameter up to which the film remained intact was measured, as specified in ISO 1519.

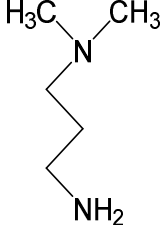
## 3. Results and Discussion

### 3.1. Synthesis and Characteristics of Compounds I–IV

Pigment Red 179 (compound I) and four new compounds (II-Mg, II-Zn, III, and IV) were synthesized for this work, and the starting component was perylene-3,4,9,10-tetracarboxy dianhydride (PTCDA). Compounds I and IV were prepared by reacting

PTCDA with the appropriate amine (Figure 3), and the reaction conditions and reaction yields are shown in Tables 1 and 2. The one-pot reactions were performed in an autoclave.

**Table 1.** Reaction conditions of preparations.

Compound	R-NH <sub>2</sub>	Reaction Conditions
I	CH <sub>3</sub> -NH <sub>2</sub>	Solvent: water Reaction temperature: 80 °C Reaction time: 4 h
IV		Solvent: water Reaction temperature: 160 °C Reaction time: 23 h

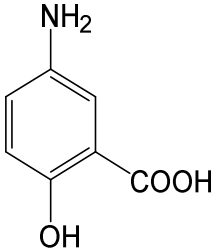
**Table 2.** Experimental yields of the preparations.

Compound	Name	Yield * (%)
I	2,9-Dimethylanthra[2,1,9-def:6,5,10-d'e'f']diisoquinoline-1,3,8,10(2H,9H)-tetraone (C <sub>26</sub> H <sub>14</sub> N <sub>2</sub> O <sub>4</sub> )	95
IV	2,9-bis(3-(Dimethylamino)propyl)anthra[2,1,9-def:6,5,10-d'e'f']diisoquinoline-1,3,8,10(2H,9H)-tetraone (C <sub>34</sub> H <sub>32</sub> N <sub>4</sub> O <sub>4</sub> )	85.3

\* Experimental yield is related to the starting PTCDA.

Compound III was prepared by a two-step synthesis in which, in the first step, the anhydride ring was opened by the reaction with KOH and the resulting intermediate was subsequently reacted with an amine (Figure 5). The reaction conditions and reaction yield are shown in Tables 3 and 4. The synthesis was performed in the one-pot way, meaning without isolating the intermediate (potassium perylene-3,4,9,10-tetracarboxylate).

**Table 3.** Reaction conditions for the preparation of compound III.

Compound	R-NH <sub>2</sub>	Reaction Conditions
III		Solvent: water Reaction temperature: 160 °C Reaction time: 23 h

**Table 4.** Experimental yield of the preparation of compound III.

Compound	Name	Yield * (%)
III	5,5'-(1,3,8,10-tetraoxo-1,3,8,10-tetrahydroanthra[2,1,9-def:6,5,10-d'e'f']diisoquinoline-2,9-diyl)bis(2-hydroxybenzoic acid) (C <sub>38</sub> H <sub>18</sub> N <sub>2</sub> O <sub>10</sub> )	88

\* Experimental yield is related to the starting PTCDA.

Compounds II-Mg and II-Zn were also prepared by a two-step synthesis in which, in the first step, the anhydride ring was opened by a reaction with KOH, and the resulting intermediate was subsequently reacted with water-soluble Mg<sup>2+</sup> or Zn<sup>2+</sup> salt (Figure 4, Tables 5 and 6).

**Table 5.** Reaction conditions for preparations of **II-Zn** and **II-Mg**.

Compound	MeCl <sub>2</sub>	Reaction Conditions
<b>II-Mg</b>	MgCl <sub>2</sub>	Solvent: water Reaction temperature: 90 °C Reaction time: 4 h
<b>II-Zn</b>	ZnCl <sub>2</sub>	Solvent: water Reaction temperature: 90 °C Reaction time: 4 h

**Table 6.** Experimental yields of the preparations of **II-Zn** and **II-Mg**.

Compound	Name	Yield * (%)
<b>II-Mg</b>	Magnesium perylene-3,4,9,10-tetracarboxylate (C <sub>24</sub> H <sub>8</sub> O <sub>8</sub> Mg <sub>2</sub> )	90.2
<b>II-Zn</b>	Zinc perylene-3,4,9,10-tetracarboxylate (C <sub>24</sub> H <sub>12</sub> O <sub>10</sub> Zn <sub>2</sub> )	82.8

\* Experimental yield is related to the starting PTCDA.

Compound **I** is an example of a widely used commercial red high-performance pigment, which has the generic name Pigment Red 179. This high-performance color pigment belongs to the class of so-called perylene-bis-imide pigments, which are highly stable in weather but have no anti-corrosion properties. For this reason, we decided to prepare and test the anti-corrosion properties of compounds that had the same central unit: perylene. The fact that they will be used as anti-corrosion compounds must not be forgotten in the preparation of these pigments. For this reason, these compounds must be thoroughly washed with water after synthesis and filtration to remove all inorganic salts. The prepared compounds **I–IV** were pigments which were insoluble in water and insoluble in organic solvents. For this reason, the prepared pigment was characterized by the following techniques. The prepared anticorrosive pigments were characterized by means of X-ray diffraction analysis, energy-dispersive X-ray spectroscopy, and inductively coupled plasma-optical emission spectroscopy (ICP-OES). The energy-dispersive X-ray spectroscopy (EDX) analysis showed the expected magnesium and zinc signals and confirmed the existence of magnesium and zinc elements in the perylene di-metal salt **II-Mg** and **II-Zn**. The distribution of elements was clarified by the EDX results, which showed that the magnesium and zinc elements were homogeneously distributed in the whole sample.

The determination of magnesium and zinc (ICP-OES) analysis showed the expected magnesium and zinc signals and confirmed the content percent of the magnesium and zinc composition in the **II-Mg** and **II-Zn**.

The D8 ADVANCE X-ray diffractometer (XRD) patterns of **II-Mg** and **II-Zn** showed strong diffraction peaks.

### 3.2. Characterization of Pigments

The results of molecular weight, elemental analysis and metal content are listed in Table 7. X-ray powder diffraction patterns are shown in Figure 6. The stacking geometry of the crystalline phases of the perylene compounds is determined by the Coulomb interaction between charged regions of the molecules, van der Waals attraction favoring a large geometric overlap of adjacent perylene cores, and the steric hindrance introduced by side groups of different sizes. Compound **I** showed its intense characteristic peaks located at 2θ values of 10.68, 7.84, 7.28, 6.60, 3.85, 3.74, 3.51, and 3.42°, with a Scherrer particle size of 23.6 nm. Compound **II-Mg** showed its intense characteristic peaks located at 2θ values of 14.27, 10.21, 5.73, 4.59, 4.00, 3.84, and 3.52°, with a Scherrer particle size of 24.8 nm. Compound **II-Zn** showed its intense characteristic peaks located at 2θ values of 14.37, 7.15, 5.71, 4.75, 4.62, and 3.01°, with a Scherrer particle size of 31.4 nm. Compound **III** showed its intense characteristic peaks located at 2θ values of 10.73, 7.87, 7.27, 6.60, 3.73,

3.51, 3.22, and 3.16°, with a Scherrer particle size of 21.7 nm. Compound IV showed its intense characteristic peaks located at 2θ values of 19.56, 11.18, 9.38, 7.24, 5.27, 5.08, 4.31, and 3.23°, with a Scherrer particle size of 23.3 nm.

**Table 7.** Characterization of synthesized pigments.

Pigment	Molecular Weight	Elemental Analysis	Metal Content
	(g·mol <sup>-1</sup> )	(%)	(mg·kg <sup>-1</sup> )
Compound I, C <sub>26</sub> H <sub>14</sub> N <sub>2</sub> O <sub>4</sub>	418.4	C: 73.96 H: 3.27 N: 6.73	0
Compound III, C <sub>38</sub> H <sub>18</sub> N <sub>2</sub> O <sub>10</sub>	662.57	C: 67.04 H: 2.77 N: 4.21	0
Compound IV, C <sub>34</sub> H <sub>32</sub> N <sub>4</sub> O <sub>4</sub>	560.65	C: 73.08 H: 5.80 N: 9.66	0
Compound II-Mg, C <sub>24</sub> H <sub>8</sub> O <sub>8</sub> Mg <sub>2</sub>	472.93	C: 54.37 H: 2.78 Mg: 10.10	Mg: 101,010
Compound II-Zn, C <sub>24</sub> H <sub>12</sub> O <sub>10</sub> Zn <sub>2</sub>	591.13	C: 48.17 H: 2.13 Zn: 21.37	Zn: 213,700

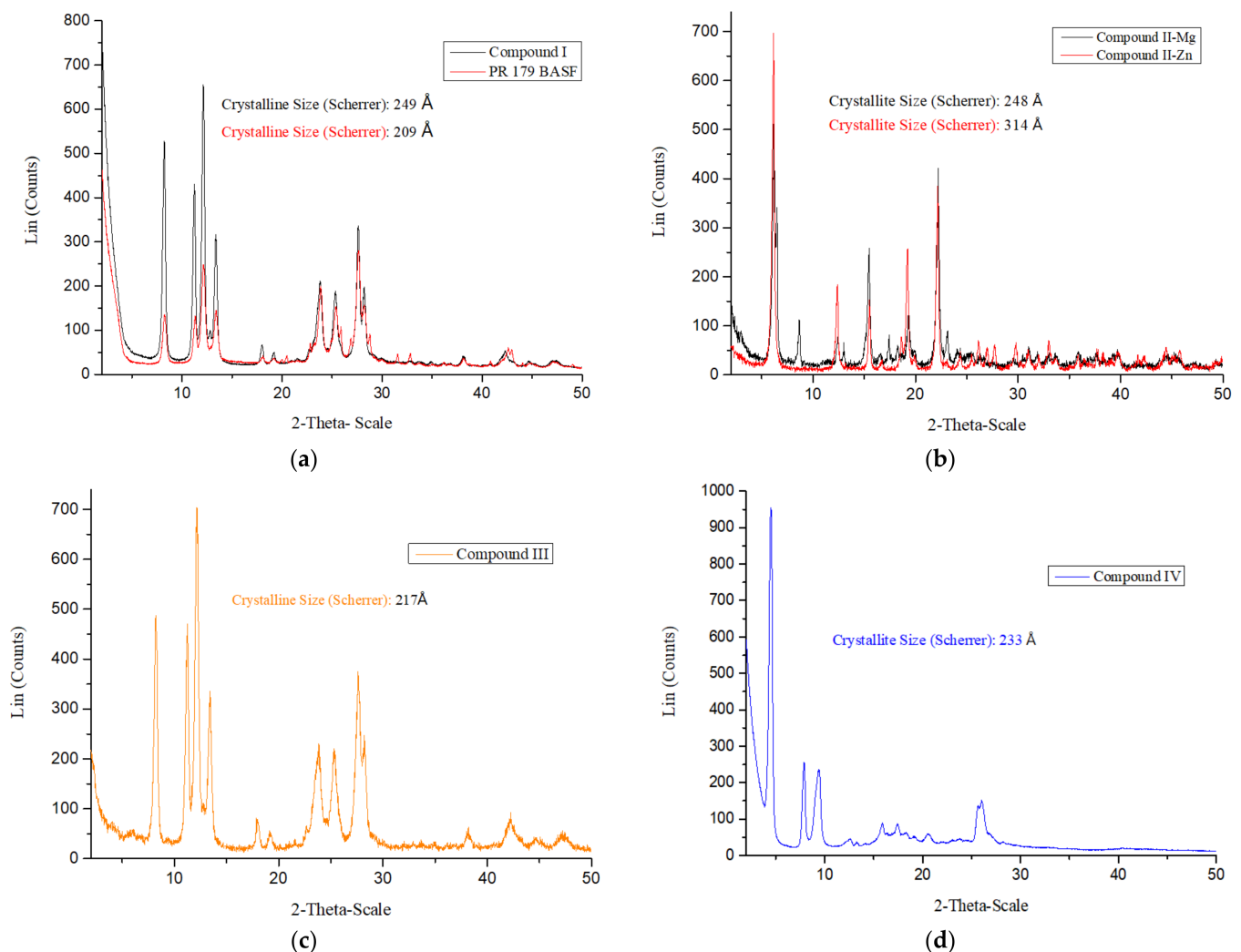


**Figure 6.** X-ray diffraction of the synthesis compounds: (a) Compound I, (b) Compound II-Zn and Compound II-Mg, (c) Compound III, and (d) Compound IV.

### 3.3. SEM: Compound IV

Scanning electron microscope (SEM) of the compound IV (a) showed homogeneity and a long crystal road with a size around 100 nm, and the compound I (b) showed granular morphology emerging with a size around 100 nm (Figure 7).

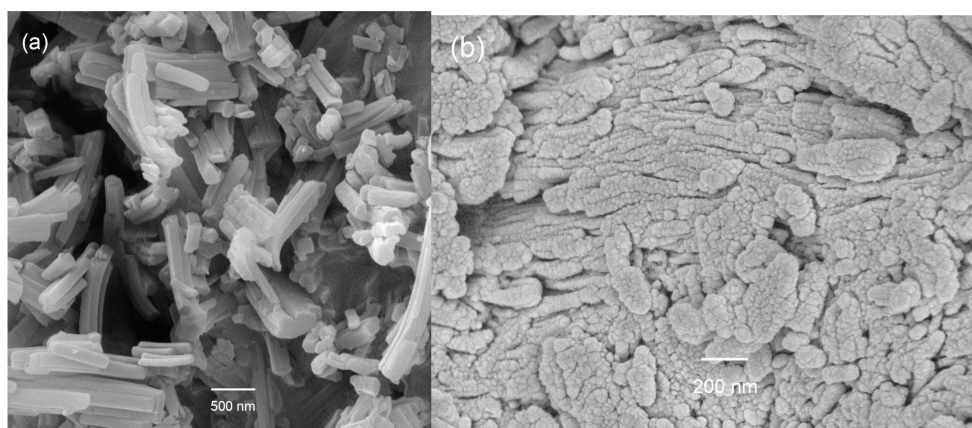


**Figure 7.** SEM of compound IV (a) and compound I (b).

### 3.4. EDX

The energy-dispersive X-ray spectroscopy (EDX) analysis showed the expected magnesium and zinc signals (Figure 8) and confirmed the existence of magnesium and zinc elements in the perylene di-metal salt compound II-Mg and compound II-Zn. The distribution of elements was clarified by the EDX results, which showed that magnesium and zinc elements were homogeneously distributed in the whole sample.

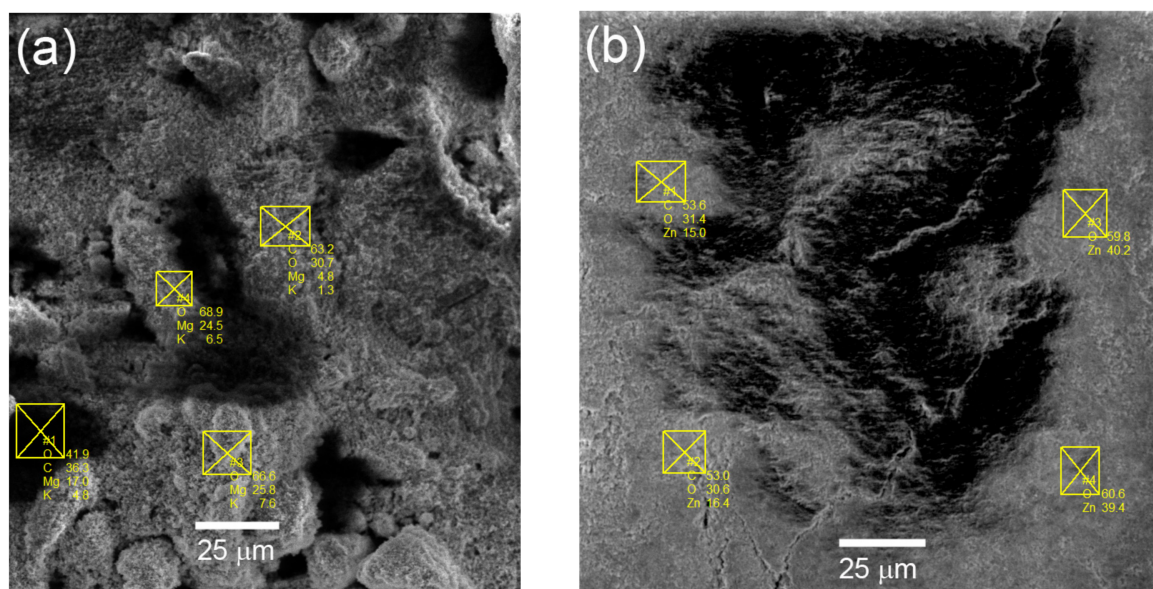


**Figure 8.** The EDX results of (a) II-Mg and (b) II-Zn showing the content of Mg and Zn in the di-salt compounds.

### 3.5. FTIR

Powders of the starting compounds PTCDA, II-Mg and II-Zn were characterized by FT-IR spectroscopy (Figure 9). The IR spectra showed slight changes between the starting compounds and the Mg and Zn complexes.

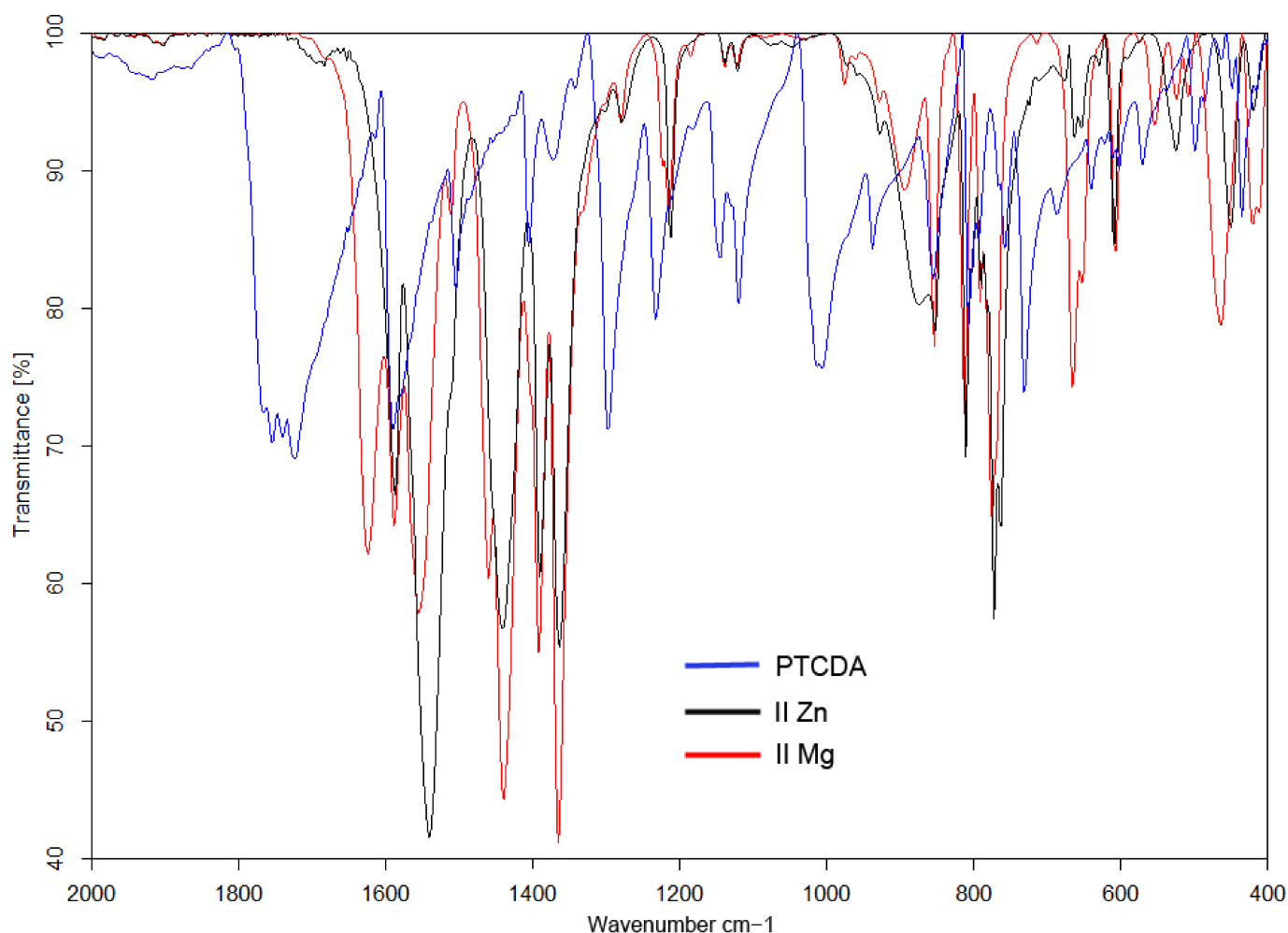


**Figure 9.** FT-IR spectra of the starting compound PTCDA (blue), compound II-Mg (red), and compound II-Zn (black).

### 3.6. Pigment Specification

The pigments, including the five perylene acid salts, were subjected to measurements of the typical paint parameters, i.e., density and oil number, which served to calculate the critical pigment volume concentration (CPVC) of each pigment. The results are listed in Table 8. The densities of both the perylene acid salts and the perylene derivative were within the range of  $1.33$  to  $1.98$   $\text{g}\cdot\text{cm}^{-3}$ ; the oil numbers were between  $64$  and  $68$   $\text{g}/100$   $\text{g}$  of the pigment; and the CPVC values were  $41$ – $52$ . Zinc nitroisophthalate density was  $2.60$   $\text{g}\cdot\text{cm}^{-3}$ , oil number was  $42$   $\text{g}/100$   $\text{g}$  of the pigment, and CPVC was  $43$ . For  $\text{TiO}_2$ , the respective values were  $4.12$   $\text{g}\cdot\text{cm}^{-3}$ ,  $27$   $\text{g}/100$   $\text{g}$  of the pigment, and  $45$ .

**Table 8.** Characteristics of the fabricated pigments: density, oil number and critical pigment volume concentration (CPVC).

Pigment	Density	Oil Absorption	CPVC
	( $\text{g}/\text{cm}^3$ )	( $\text{g}/100$ $\text{g}$ )	(-)
$\text{C}_{26}\text{H}_{14}\text{N}_2\text{O}_4$	$1.57 \pm 0.02$	65	47
$\text{C}_{38}\text{H}_{18}\text{N}_2\text{O}_{10}$	$1.56 \pm 0.02$	64	48
$\text{C}_{34}\text{H}_{32}\text{N}_4\text{O}_4$	$1.33 \pm 0.02$	65	52
$\text{C}_{24}\text{H}_8\text{O}_8\text{Mg}_2$	$1.67 \pm 0.02$	68	45
$\text{C}_{24}\text{H}_{12}\text{O}_{10}\text{Zn}_2$	$1.98 \pm 0.02$	67	41
$\text{C}_8\text{H}_5\text{NO}_6\text{-Zn}$	$2.60 \pm 0.02$	42	43
$\text{TiO}_2$	$4.12 \pm 0.02$	27	45

### 3.7. Accelerated Corrosion Tests in Atmosphere Containing SO<sub>2</sub>

All of the organic coatings examined were subjected to this cyclic test. The data in Table 9 are the results after 960 h of exposure to SO<sub>2</sub> atmosphere. Photographs of the panels after 720 h of exposure are presented in Figure 10.

**Table 9.** Results of the corrosion test performed in a condenser chamber filled with the atmosphere containing SO<sub>2</sub> with the studied organic coatings after 960 h of exposure: DFT = 70 ± 5 µm.

Pigment	PVC (%)	Blistering		Corrosion	
		Metal Base (dg)	In the Cut (dg)	In the Cut (mm)	Metal Base (%)
C <sub>38</sub> H <sub>18</sub> N <sub>2</sub> O <sub>10</sub>	0.1	8 M	6 D	1.5–2	1
	0.25	8 M	6 MD	1–1.5	0.3
	0.50	8 M	6 MD	1–1.5	0.3
C <sub>34</sub> H <sub>32</sub> N <sub>4</sub> O <sub>4</sub>	0.1	8 M	6 MD	1–1.5	0.3
	0.25	8 F	8 M	1–1.5	0.1
	0.50	8 F	8 M	1–1.5	0.1
C <sub>24</sub> H <sub>8</sub> O <sub>8</sub> Mg <sub>2</sub>	0.1	8 M	6 D	1–1.5	3
	0.25	8 F	8 M	1–1.5	0.1
	0.50	8 F	8 M	1–1.5	0.1
C <sub>24</sub> H <sub>12</sub> O <sub>10</sub> Zn <sub>2</sub>	0.1	8 F	8 M	1–1.5	0.1
	0.25	8 F	8 M	1–1.5	0.1
	0.50	8 M	6 MD	1–1.5	0.1
C <sub>8</sub> H <sub>5</sub> N <sub>0</sub> <sub>6</sub> -Zn	0.1	8 M	6 MD	1–1.5	0.3
	0.5	8 M	6 MD	1–1.5	0.3
C <sub>26</sub> H <sub>14</sub> N <sub>2</sub> O <sub>4</sub>	1	8 M	6 D	1.5–2	3
TiO <sub>2</sub>	1.5	8 MD	6 D	1.5–2	3

Neither corrosion beneath the paint film nor delamination near the artificial test cut were observed after the test for any of the coatings examined. Blisters in the cut and on the surface were observed; the number of the blisters and their size were different for the different paints and also depended on the PVC level. The resistance of the coatings to blistering with compound III at PVC = 0.25% and 0.5% was comparable to that of the paint with zinc nitroisophthalate at the PVC values used. The blisters on the surface were classed as 8M, and substrate corrosion extent was 0.3%. A higher resistance to blistering was observed with the coatings containing compound IV, C<sub>24</sub>H<sub>8</sub>O<sub>8</sub>Mg<sub>2</sub>, at PVC = 0.25% and 0.5%, and the coating containing C<sub>24</sub>H<sub>12</sub>O<sub>10</sub>Zn<sub>2</sub> at PVC = 0.1% and 0.25%. The blisters on the surface were classed as 8F, and the blisters in the cut as 8 MD. Owing to this high resistance to blistering, substrate surface corrosion was a mere 0.1%. The corrosion resistance was lower with the coating containing the pigment C<sub>26</sub>H<sub>14</sub>N<sub>2</sub>O<sub>4</sub>: the blisters in the cut were classed 6D, and the blisters on the surface were classed as 8 MD.

### 3.8. Cyclic Corrosion/Weather Resistance Test with Exposure to a Salt Electrolyte and UV Radiation

This cyclic corrosion/weather resistance test was applied to all the organic coatings studied. The data in Table 10 are the results after 1008 h of exposure. Photographs of the panels after 672 h of exposure are presented in Figure 10.

Neither corrosion beneath the paint film nor delamination near the artificial test cut were observed after the test for any of the coatings examined. Blisters in the cut and on the surface were observed; however, the number of the blisters and their size were different for the different paints and also depended on the PVC. Among the organic coatings examined, a high resistance to blistering was observed with the coating containing the C<sub>24</sub>H<sub>8</sub>O<sub>8</sub>Mg<sub>2</sub> pigment at PVC = 0.25% and 0.5%: the blisters in the cut were 6 M in degree, and blisters on the surface were 8 M. This high resistance to blistering provided a high degree of protection

for the test cut: corrosion in the cut was 2–3 mm, the lowest of the organic coatings studied. The corrosion resistance of the coating with zinc nitroisophthalate at the PVC values used was comparable. A high resistance to blistering was observed for the coatings containing the compound IV pigment: no blisters on the surface were found at PVC = 0.25% or 0.5%, and the blisters in the cut were classed as 4 M. So, these coatings provided a comparably high substrate material protection, and only the corrosion protection of the test cut had a slightly lower-corrosion in the cut attained at 3–4 mm. A lower resistance to blistering was found for the coatings containing the compound III and  $C_{24}H_{12}O_{10}Zn_2$  pigments. The corrosion resistance was also lower at any PVC value, and so the corrosion on the substrate panel surface exceeded 3%.

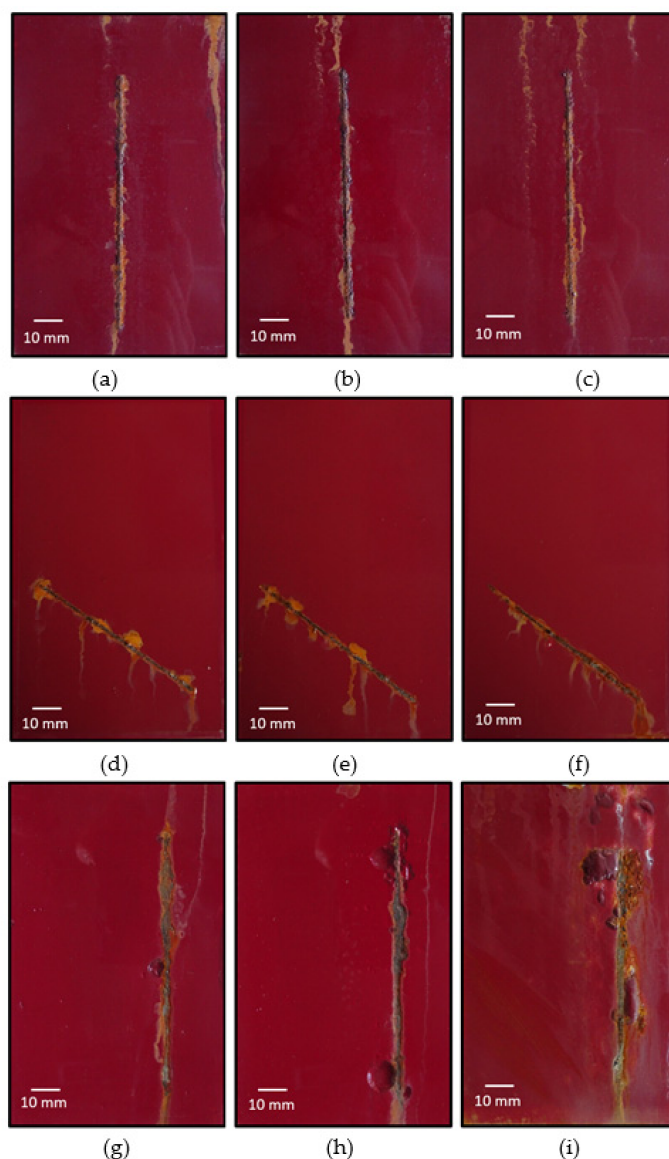


**Figure 10.** Organic coatings after 720 h of exposure in atmosphere with  $SO_2$ : (a) organic coating with  $C_{24}H_8O_8Mg_2$ , PVC = 0.5%; (b) organic coating with  $C_{24}H_{12}O_{10}Zn_2$  pigment, PVC = 0.5%; (c) organic coating with  $C_8H_5N_0_6$ -Zn pigment, PVC = 0.5%. Organic coatings after 672 h of exposure with salt electrolyte and UV radiation: (d) organic coating with  $C_{24}H_8O_8Mg_2$ , PVC = 0.5%; (e) organic coating with  $C_{24}H_{12}O_{10}Zn_2$  pigment, PVC = 0.5%; (f) organic coating with  $C_8H_5N_0_6$ -Zn pigment, PVC = 0.5%. Organic coatings after 960 h of exposure in a salt mist atmosphere: (g) organic coating with  $C_{24}H_8O_8Mg_2$ , PVC = 0.5%; (h) organic coating with  $C_{24}H_{12}O_{10}Zn_2$  pigment, PVC = 0.5%; (i) organic coating with  $C_8H_5N_0_6$ -Zn pigment, PVC = 0.5%.



**Table 10.** Results of the cyclic corrosion test in a fluorescent UV/in an atmosphere of NaCl + (NH<sub>4</sub>)<sub>2</sub>SO<sub>4</sub> with water steam condensation for the studied organic coatings after 1008 h of exposure: DFT = 70 ± 5 µm.

Pigment	PVC (%)	Blistering		Corrosion	
		Metal Base (dg)	In the Cut (dg)	In the Cut (mm)	Metal Base (%)
C <sub>38</sub> H <sub>18</sub> N <sub>2</sub> O <sub>10</sub>	0.1	8 M	4 MD	3–4	3
	0.25	8 MD	4 MD	3–4	10
	0.50	8 D	4 MD	3–4	16
C <sub>34</sub> H <sub>32</sub> N <sub>4</sub> O <sub>4</sub>	0.1	8 F	4 M	2–3	0.3
	0.25	-	4 M	3–4	0.3
	0.50	-	4 M	3–4	0.3
C <sub>24</sub> H <sub>8</sub> O <sub>8</sub> Mg <sub>2</sub>	0.1	8 F	6 M	2–3	1
	0.25	8 M	6 M	2–3	0.3
	0.50	8 M	6 M	2–3	0.3
C <sub>24</sub> H <sub>12</sub> O <sub>10</sub> Zn <sub>2</sub>	0.1	8 MD	6 M	3–4	3
	0.25	8 MD	6 M	3–4	3
	0.50	8 D	6 MD	3–4	16
C <sub>8</sub> H <sub>5</sub> N <sub>0</sub> <sub>6</sub> -Zn	0.1	-	6 M	2–3	0.3
	0.5	6 F	4 M	2–3	0.3
C <sub>26</sub> H <sub>14</sub> N <sub>2</sub> O <sub>4</sub>	1	4 F	2 MD	5–6	0.3
TiO <sub>2</sub>	1.5	4 M	6 M	3–4	0.3

### 3.9. Accelerated Corrosion Tests in a Salt Mist Atmosphere

This cyclic corrosion test was applied to all the organic coatings studied. The data in Table 11 are the results after 1440 h of exposure to a salt fog atmosphere. Photographs of the panels after 960 h of exposure are presented in Figure 10.

**Table 11.** Results of the corrosion test performed in a salt mist chamber of the studied organic coatings after 1441 h of exposure: DFT = 70 ± 5 µm.

Pigment	PVC (%)	Blistering		Corrosion	
		Metal Base (dg)	In the Cut (dg)	In the Cut (mm)	Metal Base (%)
C <sub>38</sub> H <sub>18</sub> N <sub>2</sub> O <sub>10</sub>	0.1	6 M	2 MD	4–5	1
	0.25	6 M	2 MD	4–5	1
	0.50	6 M	2 M	2–3	1
C <sub>34</sub> H <sub>32</sub> N <sub>4</sub> O <sub>4</sub>	0.1	6 M	2 D	4–5	0.3
	0.25	6 MD	2 MD	4–5	0.3
	0.50	6 M	2 M	2–3	0.3
C <sub>24</sub> H <sub>8</sub> O <sub>8</sub> Mg <sub>2</sub>	0.1	8 M	4 M	2–3	0.3
	0.25	8 M	2 M	2–3	0.1
	0.50	8 M	2 M	2–3	0.1
C <sub>24</sub> H <sub>12</sub> O <sub>10</sub> Zn <sub>2</sub>	0.1	6 MD	2 MD	3–4	0.3
	0.25	6 MD	2 MD	3–4	0.3
	0.50	6 MD	2 M	3–4	0.3
C <sub>8</sub> H <sub>5</sub> N <sub>0</sub> <sub>6</sub> -Zn	0.1	6 M	2 M	3–4	0.3
	0.5	6 MD	2 M	2–3	0.3
C <sub>26</sub> H <sub>14</sub> N <sub>2</sub> O <sub>4</sub>	1	6 MD	2 D	5–6	1
TiO <sub>2</sub>	1.5	6 MD	2 D	7–8	3

No corrosion beneath the paint film was observed for any of the coatings after the 1440 h exposure. Blisters in the cut and on the surface were observed, and the number of blisters and their size were different for the different paints, and also depended on the PVC. A high resistance to blistering after the 1440 h exposure was observed for the coating with zinc nitroisophthalate at PVC = 0.5%: the blisters on the paint film surface and in the cut were classed as 6 MD and 2 M, respectively. Owing to this high resistance to blistering, the corrosion on the panel surface was a mere 0.3% and the corrosion in the cut did not exceed 3 mm. A high corrosion resistance was also observed for the coatings containing the PDA-DMAPA pigment. The blisters on the paint film surface and in the cut were classed as 6 M and 2 M, respectively. The highest corrosion resistance was observed for the coatings containing the  $C_{24}H_8O_8Mg_2$  pigment at PVC = 0.25 and 0.5%: the blisters on the paint film surface and in the cut were 8 M and 2 M in degree, respectively. Owing to this high resistance to blistering, these coatings provided corrosion protection to the steel substrate: corrosion on the panel surface was a mere 0.1%, and corrosion in the cut did not exceed 3 mm. The remaining organic coatings exhibited a lower resistance to blistering, due to which the corrosion on the substrate panel surface was more marked, attaining 0.3% to 3%.

### 3.10. Potentiodynamic Polarization Studies

Each of the organic coatings were also subjected to the electrochemical linear polarization test. The results are presented in Table 12. This test was also applied to the samples that had been subjected to the 480 h  $SO_2$  atmosphere exposure (Table 13).

**Table 12.** Results of the electrochemical test in a 1 M NaCl solution of the organic coatings, DFT =  $60 \pm 5 \mu m$ .

Pigment	PVC (%)	$E_{corr}$ (mV)	$I_{corr}$ ( $\mu A$ )	$\beta_a$ (mV)	$\beta_c$ (mV)	$R_p$ ( $\Omega$ )	$v_{corr}$ ( $mm\ year^{-1}$ )
$C_{38}H_{18}N_2O_{10}$	0.1	−193	$0.4 \times 10^{-3}$	16.1	19.9	$9.78 \times 10^6$	$53.1 \times 10^{-7}$
	0.25	−123	$0.1 \times 10^{-3}$	40.2	32.7	$7.62 \times 10^6$	$19.9 \times 10^{-7}$
	0.50	−246	$0.2 \times 10^{-3}$	16.6	19.0	$9.65 \times 10^6$	$30.5 \times 10^{-7}$
$C_{34}H_{32}N_4O_4$	0.1	−330	$0.8 \times 10^{-4}$	22.6	23.0	$5.76 \times 10^7$	$11.5 \times 10^{-7}$
	0.25	−555	$0.7 \times 10^{-4}$	42.2	42.0	$6.75 \times 10^7$	$19.2 \times 10^{-7}$
	0.50	−368	$0.7 \times 10^{-4}$	21.8	22.9	$4.68 \times 10^7$	$12.8 \times 10^{-7}$
$C_{24}H_8O_8Mg_2$	0.1	−451	$0.3 \times 10^{-4}$	28.9	24.3	$2.21 \times 10^8$	$36.9 \times 10^{-8}$
	0.25	−354	$0.1 \times 10^{-4}$	35.2	33.6	$6.86 \times 10^8$	$14.8 \times 10^{-8}$
	0.50	−440	$0.1 \times 10^{-4}$	33.6	39.0	$6.44 \times 10^8$	$14.1 \times 10^{-8}$
$C_{24}H_{12}O_{10}Zn_2$	0.1	−415	$0.2 \times 10^{-4}$	20.0	15.1	$1.66 \times 10^8$	$28.5 \times 10^{-8}$
	0.25	−563	$0.1 \times 10^{-4}$	26.7	14.7	$3.75 \times 10^8$	$16.2 \times 10^{-8}$
	0.50	−486	$0.2 \times 10^{-4}$	22.6	23.8	$3.68 \times 10^8$	$16.8 \times 10^{-8}$
$C_8H_5N_0_6-Zn$	0.1	−145	$0.4 \times 10^{-3}$	38.6	30.2	$5.44 \times 10^6$	$93.2 \times 10^{-7}$
	0.5	−428	$0.5 \times 10^{-3}$	42.7	31.3	$1.51 \times 10^7$	$76.4 \times 10^{-7}$
$C_{26}H_{14}N_2O_4$	1	−331	$0.1 \times 10^{-2}$	32.1	25.5	$5.54 \times 10^6$	$14.8 \times 10^{-6}$
$TiO_2$	1.5	−357	$0.2 \times 10^{-2}$	33.8	33.2	$3.41 \times 10^5$	$29.5 \times 10^{-5}$

The PCVs of the newly studied pigments for application with organic binder in the coating were chosen at low values (0.1, 0.25 and 0.5%). The reason was that these were pigments of an organic nature with a presumed anti-corrosion effect, which are standardly dosed at low concentrations, usually up to PVC = 1%. Unlike metallic protective coatings, at such low concentrations of the anticorrosive component of the organic coating, the spontaneous corrosion potential ( $E_{corr}$ ) slowly stabilizes. The values of spontaneous corrosion potential for these types of coatings oscillate over a wider range. A similar dependence was found in the determination of  $\beta_a$  and  $\beta_c$  parameters; however, the results of the determined polarization resistances and corrosion rates of individual studied organic coatings corresponded to the results of the cyclic corrosion tests. Figure 11 shows that, in the steel panels,

after removing the organic coating with the pigment content  $C_{24}H_8O_8Mg_2$  at PVC = 0.5%, corrosion in the area reached only 0.3% ( $R_p = 2.95 \times 10^7 \Omega$ ,  $v_{corr} = 17.9 \times 10^{-7} \text{ mm}\cdot\text{year}^{-1}$ ), while corrosion in the area reached 1% ( $R_p = 9.65 \times 10^4 \Omega$ ,  $v_{corr} = 13.3 \times 10^{-4} \text{ mm}\cdot\text{year}^{-1}$ ) after removing the coating containing the pigment  $C_{38}H_{18}N_2O_{10}$  (PR 179) at PVC = 1%.

**Table 13.** Results of the electrochemical test in a 1M NaCl solution for the organic coatings after 480 h of exposure in atmosphere containing  $SO_2$ : DFT =  $60 \pm 5 \mu\text{m}$ .

Pigment	PVC (%)	$E_{corr}$ (mV)	$I_{corr}$ ( $\mu\text{A}$ )	$\beta_a$ (mV)	$\beta_c$ (mV)	$R_p$ ( $\Omega$ )	$v_{corr}$ ( $\text{mm year}^{-1}$ )
$C_{38}H_{18}N_2O_{10}$	0.1	−490	$0.5 \times 10^{-1}$	46.2	52.8	$2.20 \times 10^5$	$69.4 \times 10^{-5}$
	0.25	−523	$0.4 \times 10^{-1}$	45.8	50.6	$3.14 \times 10^5$	$58.2 \times 10^{-5}$
	0.50	−563	$0.2 \times 10^{-1}$	43.3	46.1	$5.52 \times 10^5$	$25.1 \times 10^{-5}$
$C_{34}H_{32}N_4O_4$	0.1	−489	$0.5 \times 10^{-1}$	42.6	39.6	$2.28 \times 10^5$	$73.3 \times 10^{-5}$
	0.25	−491	$0.4 \times 10^{-1}$	43.2	45.7	$3.62 \times 10^5$	$69.2 \times 10^{-5}$
	0.50	−499	$0.3 \times 10^{-1}$	42.8	43.6	$4.12 \times 10^5$	$48.9 \times 10^{-5}$
$C_{24}H_8O_8Mg_2$	0.1	−522	$0.9 \times 10^{-2}$	39.6	39.1	$1.22 \times 10^6$	$10.3 \times 10^{-6}$
	0.25	−513	$0.1 \times 10^{-3}$	26.2	24.8	$3.65 \times 10^7$	$17.8 \times 10^{-7}$
	0.50	−518	$0.1 \times 10^{-3}$	21.3	16.5	$2.95 \times 10^7$	$17.9 \times 10^{-7}$
$C_{24}H_{12}O_{10}Zn_2$	0.1	−487	$0.3 \times 10^{-1}$	43.6	44.1	$2.02 \times 10^5$	$35.9 \times 10^{-5}$
	0.25	−496	$0.1 \times 10^{-2}$	42.1	43.8	$6.17 \times 10^6$	$11.6 \times 10^{-6}$
	0.50	−498	$0.2 \times 10^{-2}$	40.8	41.6	$2.21 \times 10^6$	$23.2 \times 10^{-6}$
$C_8H_5N_0_6-Zn$	0.1	−189	$0.1 \times 10^{-2}$	38.2	36.3	$3.63 \times 10^6$	$11.6 \times 10^{-6}$
	0.5	−398	$0.4 \times 10^{-2}$	38.3	34.8	$1.34 \times 10^6$	$46.8 \times 10^{-6}$
$C_{26}H_{14}N_2O_4$	1	−470	$0.9 \times 10^{-2}$	42.3	37.9	$9.65 \times 10^4$	$13.3 \times 10^{-4}$
$TiO_2$	1.5	−401	$0.9 \times 10^{-1}$	30.5	41.2	$4.12 \times 10^3$	$10.3 \times 10^{-3}$

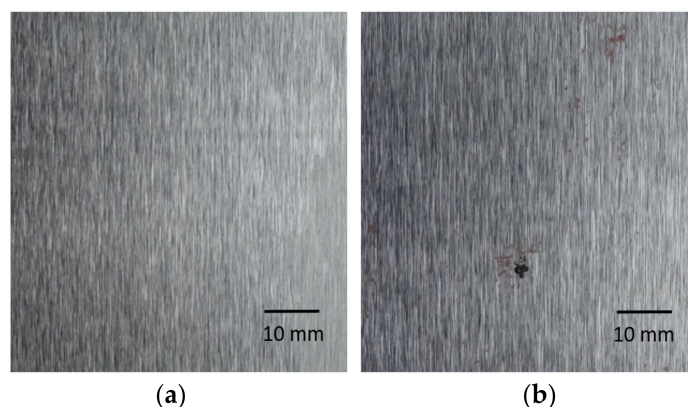


**Figure 11.** Steel panels after removing the organic coating: (a) pigment  $C_{24}H_8O_8Mg_2$ , PVC = 0.5%, atmosphere containing  $SO_2$ ; (b) pigment  $C_{38}H_{18}N_2O_{10}$ , PVC = 1%, atmosphere containing  $SO_2$ .

The polarization resistance and corrosion rates of the coatings with compound IV at the PVC values used were comparable to those of the coating pigmented with zinc nitroisophthalate at PVC = 0.5%. Polarization resistances one order of magnitude higher and, at the same time, corrosion rates one order of magnitude lower were observed with the coatings containing the  $C_{24}H_8O_8Mg_2$  and  $C_{24}H_{12}O_{10}Zn_2$  pigments, respectively, for all of the PVC values used. The polarization curves were also measured for the coatings on the panels that had been exposed to the  $SO_2$  atmosphere for 480 h and exhibited no blisters, no corrosion on the steel substrate surface, and no other paint film degradation signs. Decreases in polarization resistance and increases in corrosion rate were observed for all of them. Nevertheless, the order of the corrosion resistance among the coatings remained unchanged: the highest polarization resistance values and lowest corrosion rates were

found for the coatings with the  $C_{24}H_8O_8Mg_2$  pigment at PVC = 0.25 and 0.5%, although the data were one order of magnitude poorer than those of the same coatings that had not been exposed to the aggressive atmosphere.

3.11. Evaluation of Mechanical Tests

All the coatings were subjected to mechanical tests to examine their mechanical resistance. The dry film thickness was  $60 \pm 5 \mu m$ . The result of the adhesion test was 0, since all the cuts were smooth and no peel-off was observed. None of the paint films were disturbed by bending over a cylindrical mandrel 4 mm in diameter, or by the impact of a 1kg weight on either of the panel sides from a 1 m height, or even by the cupping test where the test body penetrated to a 10 mm depth. In conclusion, the presence of any of the pigments did not affect adversely the mechanical resistance of the organic coating (the mechanical values were no poorer than those of the non-pigmented coating).

3.12. Assumed Mechanism of Action of the Perylene Acid Salts in the Organic Coatings

The results showed that the highest corrosion resistance during the cyclic corrosion tests was attained with the coating containing  $C_{24}H_8O_8Mg_2$  at concentrations of 0.25 and 0.5 wt.%, in comparison to the coatings containing  $C_{26}H_{14}N_2O_4$  or  $C_8H_5N_0_6-Zn$  (the commercial corrosion inhibitor). The electrochemical linear polarization tests gave the same result. It can be concluded that the perylene acid salt pigments, particularly the  $C_{24}H_8O_8Mg_2$  type, are able to help inhibit corrosion effects to the extent that they are superior to the commonly used corrosion inhibitors of the zinc nitroisophthalate type.

The mechanism of action of the pigment types (Figures 12 and 13) in question is based on their ability to form complexes at the metallic surface/pigmented organic coating/corrosive medium interface. It has also been demonstrated that hydrolysis and re-complexation give rise the formation of the molecular divalent metal oxide, which can react to provide metal hydroxide. Subsequently, this hydroxide may neutralize any acids that accelerate corrosion, and form a protective layer on the steel surface. The perylene acid salts also act as an anodic anticorrosion pigment/inhibitor forming an insoluble protective film on the anode surface (corrosion microcell) and passivating it. Additionally,  $\pi$  systems are known to have affinity for iron owing to the formation of 'π bonds', where the layer on the iron surface need not necessarily be monomolecular owing to the existence of  $\pi-\pi$  stacking between the  $\pi$  systems.

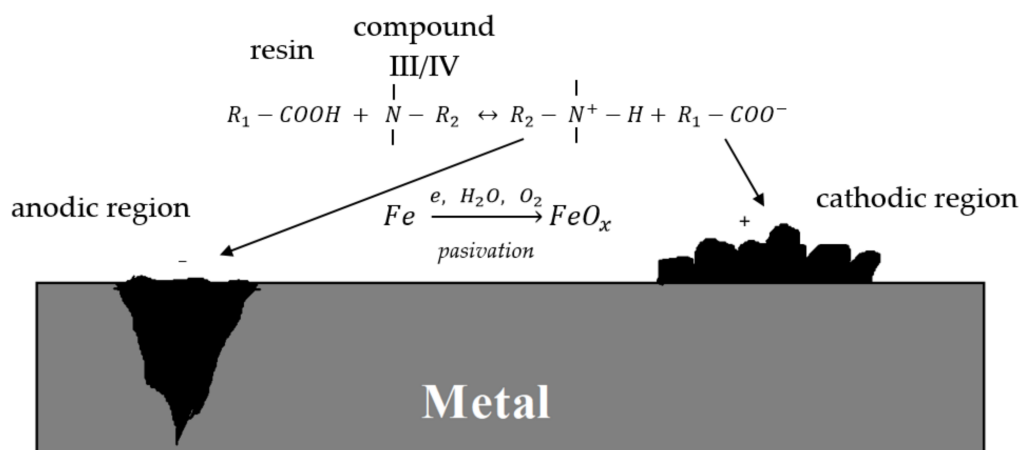
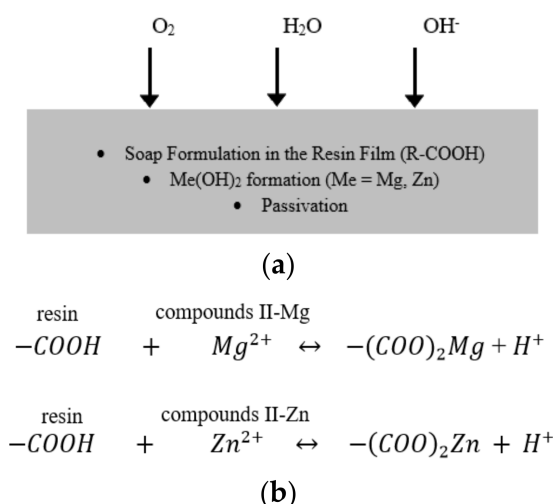


Figure 12. Schematic representation of the proposed protective mechanism of compound III and compound IV.



**Figure 13.** Schematic representation of the proposed protective mechanism (a) of compound II–Mg and compound II–Zn (b).

Furthermore, the mechanical test results demonstrate that the pigments do not adversely affect the mechanical resistance of the base coating: the mechanical resistance of the pigmented organic coatings attained maximum levels and so, the coatings can be recommended for stressed mechanical structures.

#### 4. Conclusions

The objective of this work was to synthesize and describe the new perylene acid  $Mg^{2+}$  and  $Zn^{2+}$  salts, and also the perylene bis-immide derivatives of perylene, to study their anticorrosion capacity when used as pigments in epoxy ester resin-based coatings. The set of compounds I, II–Zn, II–Mg, III and IV was successfully prepared and characterized by analytical methods (SEM, EDX, X-ray). The results of both the cyclic corrosion tests and electrochemical linear polarization measurements gave evidence of a high anticorrosion strength resistance of the perylene acid salts  $C_{24}H_{12}O_{10}Zn_2$  and  $C_{24}H_8O_8Mg_2$  at pigment volume concentrations of 0.25% and 0.5%. Their mechanism of action was mainly in their complexation capacity at the metal surface/organic coating/corrosive medium interface.

We compared the test results from the simulated corrosion tests in the atmosphere containing NaCl or  $SO_2$  with the electrochemical method of measurement by linear polarization. Out of all the compounds, pigments with Zn and Mg salts (i.e., di-magnesium salt of perylene-3,4,9,10-tetracarboxylic acid ( $C_{24}H_8O_8Mg_2$ ) and the dizinc salt of perylene-3,4,9,10-tetracarboxylic acid ( $C_{24}H_{12}O_{10}Zn_2$ )) had higher corrosion protection of the metal substrate, and the protection against blistering in the coating was excellent compared to the pigments without Mg or Zn ( $C_{38}H_{18}N_2O_{10}$ ) and ( $C_{34}H_{32}N_4O_4$ ).

Furthermore, coatings containing the pigment perylene acid  $Mg^{2+}$  (dimagnesium salt of perylene-3,4,9,10-tetracarboxylic acid  $C_{24}H_8O_8Mg_2$ ) showed a higher corrosion inhibitory effect, which was demonstrated by electrochemical tests compared to coatings containing perylene acid  $Zn^{2+}$  (dizinc salt of perylene-3,4,9,10-tetracarboxylic acid ( $C_{24}H_{12}O_{10}Zn_2$ )). The decrease in value in the corrosion rates ( $v_{corr}$ ) of coatings containing the pigment  $C_{24}H_8O_8Mg_2$  was lower after 480 h exposure in an atmosphere containing  $SO_2$  (reduction in the corrosion rate by one to two orders of magnitude) than in the case of the coating containing the pigment  $C_{24}H_{12}O_{10}Zn_2$  (reduction in the corrosion rate by two to three orders of magnitude) compared to the values of corrosion rates measured before the exposure of the samples in the above test. This conclusion was also confirmed by the evaluation of the measured polarization resistance ( $R_p$ ). In the case of the pigment  $C_{24}H_8O_8Mg_2$ , the protective mechanism was enhanced by the formation of a more chemically active basic  $Mg(OH)_2$ .

Mechanical tests gave evidence that the perylene-type pigments had no adverse effects on the systems' mechanical properties: the mechanical resistance attained maximum levels.

## 5. Patent

This work is partly published as patent No: CZ308991B6, Hrdina R., Burgert L., Kalendová A., Alafid F., Panák O., Držková M. and Kohl M: Use of salts of perylenic acid as anticorrosive substances. CZ308991B6, 2021.

**Author Contributions:** Conceptualization, M.K., F.A., A.K. (Andréa Kalendová) and R.H.; methodology, M.K., F.A., Y.R., M.B. and A.K. (Anna Krejčová); software, M.K. and F.A.; validation, M.K. and F.A.; formal analysis, M.K., F.A., M.B., A.K. (Anna Krejčová) and A.K. (Andréa Kalendová); investigation, M.K. and F.A.; resources, M.K. and F.A.; data curation, M.K. and F.A.; writing—original draft preparation, M.K. and F.A.; writing—review and editing, M.K., F.A., A.K. (Andréa Kalendová), Y.R. and R.H.; visualization, M.K. and F.A.; supervision, A.K. (Andréa Kalendová), R.H. and L.B. All authors have read and agreed to the published version of the manuscript.

**Funding:** This work was supported by the grant TRIO program, Ministry of Industry and Trade, Czech Republic, project MPO TRIO FV30048.

**Institutional Review Board Statement:** Not applicable.

**Informed Consent Statement:** Not applicable.

**Data Availability Statement:** Not applicable.

**Conflicts of Interest:** The authors declare no conflict of interest.

## References

1. Zmozinski, A.V.; Peres, R.S.; Freiburger, K.; Ferreira, C.A.; Tamborim, S.M.M.; Azambuja, D.S. Zinc tannate and magnesium tannate as anticorrosion pigments in epoxy paint formulations. *Progress Org. Coat.* **2018**, *21*, 23–29. [[CrossRef](#)]
2. Sørensen, P.A.; Kiil, S.; Dam-Johansen, K.; Weinell, C.E. Anticorrosive coatings: A review. *J. Coat. Technol. Res.* **2009**, *6*, 135–176. [[CrossRef](#)]
3. Naderi, R.; Mahdavian, M.; Darvish, A. Electrochemical examining behavior of epoxy coating incorporating zinc-free phosphate-based anticorrosion pigment. *Progress Organic Coatings* **2013**, *76*, 302–306. [[CrossRef](#)]
4. Benda, P.; Kalendová, A. Anticorrosion properties of pigments based on ferrite coated zinc particles. *Phys. Procedia* **2013**, *44*, 185–194. [[CrossRef](#)]
5. Xue, Y.N.; Xue, X.Z.; Miao, M.; Liu, J.K. Mass preparation and anticorrosion mechanism of highly triple-effective corrosion inhibition performance for co-modified zinc phosphate-based pigments. *Dyes Pigments* **2019**, *161*, 489–499. [[CrossRef](#)]
6. Griffiths, C.M.; Wint, N.; Williams, G.; McMurray, H.N. The contribution of Zn(II) and phosphate anions to the inhibition of organic coating cathodic disbondment on galvanised steel by zinc phosphate pigment. *Corros. Sci.* **2022**, *198*, 110111. [[CrossRef](#)]
7. Darvish, A.; Naderi, R.; Attar, M.M. The impact of pigment volume concentration on the protective performance of polyurethane coating with second generation of phosphate based anticorrosion pigment. *Progress Org. Coat.* **2014**, *77*, 1768–1773. [[CrossRef](#)]
8. Ghali, E.; Sastri, V.S.; Elboudjaini, M. *Corrosion Prevention and Protection: Practical Solutions*; John Wiley & Sons, Ltd.: Hoboken, NJ, USA, 2007; ISBN 978-0-470-02402-7.
9. Černý, L.; Němcová, J. *Inhibitory Korozě Kovů*; SNTL: Prague, Czech Republic, 1964.
10. Miao, M.; Yuan, X.Y.; Wang, X.G.; Lu, Y.; Liu, J.K. One step self-heating synthesis and their excellent anticorrosion performance of zinc phosphate/benzotriazole composite pigments. *Dyes Pigments* **2017**, *141*, 74–82. [[CrossRef](#)]
11. Ramezanzadeh, B.; Ghasemi, E.; Askari, F.; Mah, M. Synthesis and characterization of a new generation of inhibitive pigment based on zinc acetate/benzotriazole: Solution phase and coating phase studies. *Dyes Pigments* **2015**, *122*, 331–345. [[CrossRef](#)]
12. Kreislová, K. Inhibitory korozě. *Korozě Ochrana Mater.* **1996**, *40*, 25–29.
13. Cervová, J.; Hagarová, M. The impact of corrosion inhibitors on the effectiveness of metallic materials corrosion protection. *Korozě Ochrana Mater.* **2013**, *56*, 1–5. [[CrossRef](#)]
14. Eduok, U.; Faye, O.; Szpunar, J.; Khaled, M. CS<sub>2</sub> mediated synthesis of corrosion-inhibiting mercaptobenzothiazole molecule for industrial zinc: Experimental studies and molecular dynamic simulations. *J. Mol. Liquids* **2021**, *324*, 115129. [[CrossRef](#)]
15. Adams, R. Heubach keeps adding to its family of organic & inorganic pigments. *Focus Pigments* **2005**, *10*, 1–4.
16. Zhang, T.; Zagranjarsk, I.Y.; Skabeev, A.; Müllen, K.; Li, C. Perylene pigments as alternatives to phthalocyanine and indanthrone blue. *Dyes Pigments* **2021**, *196*, 109780. [[CrossRef](#)]
17. Ren, R.Y.; Yang, L.; Han, J.L.; Cheng, H.Y.; Ajibade, F.O.; Guadie, A.; Wang, H.C.; Liu, B.; Wang, A.J. Perylene pigment wastewater treatment by fenton-enhanced biological process. *Environ. Res.* **2020**, *186*, 109522. [[CrossRef](#)]
18. Suzuki, E.M. Infrared spectra of North American automobile original finishes. X: Analysis of perylene pigments—In situ identification of Perylene Red Y (C.I. Pigment Red 224) and mica-based red pearlescent pigments. *Forensic Chem.* **2021**, *25*, 100350. [[CrossRef](#)]
19. Kopřivová, P. Evaluation of Modified Developmental Types of Biodegradable Chelating Surfactants and Sequestering Agents. Master's Thesis, University of Pardubice, Pardubice, Czech Republic, 2015.
20. Stohr, A.; Uschmann, H.J. Verfahren zur Herstellung von Pigment Rot 149. European Patent 2113012 B1, 28 August 2008.

21. Schulz, G.R. Perylene Pigment Composition. U.S. Patent 006391104B1, 21 May 2002.
22. Schulz, G.R.; Greene, M.J. Process For The Preparation Of Highly Chromatic Perylene Pigments. European Patent 1020496 A1, 19 July 2000.
23. Henning, G.; Blaschka, P. N,N'-Dimethylperylene-3,4,9,10-tetracarboxylic acid diimide pigments suitable for water-based paints. The synthesis of the PR 179 was done by the following above patents, but with minor modification. U.S. Patent 006099636A, 21 March 2000.
24. Zhao, J.; Su, P.; Zhao, Y.; Li, M.; Yang, Y.; Yang, Q.; Li, C. Systematic morphology and phase control of Mg-ptcda coordination polymers by Ostwald ripening and self-templating. *J. Mater. Chem.* **2012**, *22*, 8470–8475. [[CrossRef](#)]
25. Zhao, J.; Zhang, Y.; Su, P.; Jiang, Z.; Yang, Q.; Li, C. Preparation of Zn–Co–O mixed–metal oxides nanoparticles through a facile coordination polymer–based process. *RSC Adv.* **2013**, *3*, 4081–4085. [[CrossRef](#)]
26. Maki, T.; Hashimoto, H. Vat Dyes of Acenaphthene Series VI. Derivatives of Acenaphthene Violet1. *Bull. Chem. Soc. Jpn.* **1954**, *27*, 602–605. [[CrossRef](#)]
27. Zhao, Z.; Niu, F.; Li, P.; Wang, H.; Zhang, Z.; Meyer, G.J.; Hu, K. Visible Light Generation of a Microsecond Long-Lived Potent Reducing Agent. *J. Am. Chem. Soc.* **2022**, *144*, 7043–7047. [[CrossRef](#)]
28. Franke, D.; Vos, M.; Antonietti, M.; Sommerdijk, N.; Faul, C. Induced Supramolecular Chirality in Nanostructured Materials: Ionic Self-Assembly of Perylene-Chiral Surfactant Complexes. *Chem. Mater.* **2006**, *18*, 1839–1847. [[CrossRef](#)]
29. Hrdina, R.; Burgert, L.; Kalendová, A.; Alafid, F.; Panák, O.; Držková, M.; Kohl, M. Use of Salts of Perylenic Acid as Anticorrosive Substances. CZ308991B6, 29 September 2021.
30. Chen, J.; Jiao, H.; Li, W.; Liao, D.; Zhou, H.; Yu, C. Real-Time Fluorescence Turn-On Detection of Alkaline Phosphatase Activity with a Novel Perylene Probe. *Chem. Asian J.* **2013**, *8*, 276–281. [[CrossRef](#)] [[PubMed](#)]
31. Ma, T.; Li, C.; Shi, G. Optically Active Supramolecular Complex Formed by Ionic Self-Assembly of Cationic Perylene diimide Derivative and Adenosine Triphosphate. *Langmuir* **2008**, *24*, 43–48. [[CrossRef](#)] [[PubMed](#)]
32. Kohl, M.; Kalendová, A. Assessment of the impact of polyaniline salts on corrosion properties of organic coatings. *Koroze Ochrana Mater.* **2014**, *58*, 113–119. [[CrossRef](#)]
33. Toshev, Y.; Mandova, V.; Boshkov, N.; Stoychev, D.; Petrov, P.; Tsvetkova, N.; Raichevski, G.; Tsvetanov, C.; Gabev, A.; Velev, R.; et al. Protective coating of zinc and zinc alloys for industrial applications. In Proceedings of the 4M 2006—Second International Conference on Multi-Material Micro Manufacture, Grenoble, France, 20–22 September 2006; pp. 323–326.
34. Kouřil, M.; Novák, P.; Bojko, M. Limitations of the linear polarization method to determine stainless steel corrosion rate in concrete environment. *Cement Concr. Compos.* **2006**, *28*, 220–225. [[CrossRef](#)]
35. Kalendová, A.; Veselý, D. Study of the anticorrosive efficiency of zincite and periclase-based core–shell pigments in organic coatings. *Progress Org. Coat.* **2009**, *64*, 5–19. [[CrossRef](#)]
36. Millard, S.G.; Law, D.; Bungey, J.H.; Cairns, J. Environmental influences on linear polarisation corrosion rate measurement in reinforced concrete. *NDT E Int.* **2001**, *34*, 409–417. [[CrossRef](#)]